Durability of concrete made with recycled concrete aggregates after exposure to elevated temperatures

Bruno Fernandes, Michel Khodeir, Céline Perlot-Bascoules, Hélène Carré, Jean-Christophe Mindeguia, Christian La Borderie

Durability of concrete made with recycled concrete aggregates after exposure to elevated temperatures

Bruno Fernandes[1*†], Michel Khodeir[1†], Céline Perlot[1,2†], Hélène Carré[1†], Jean-Christophe Mindeguia[3†] and Christian La Borderie[1†]

[1]SIAME, E2S UPPA, Université de Pau et des Pays de l'Adour, Allée du Parc Montaury, Anglet, 64600, France.
[2]Institut Universitaire de France (IUF).
[3]Laboratoire l2M, Université de Bordeaux, Cours de la Libération, Talence, 33405, France.

*Corresponding author(s). E-mail(s): b.fernandes@leeds.ac.uk;
†These authors contributed equally to this work.

Abstract

The behaviour of concrete made with recycled concrete aggregates (RCA) at room temperature is well-studied. However, some points still need to be addressed, especially in extreme conditions such as durability and high temperature. This paper evaluates the effect of elevated temperatures on the durability of concrete made with RCA. Three concrete mixes were studied: concrete with NA (reference), 100 % direct replacement (DR) mix (RCA-100-DR) and 100 % strength-based replacement (SBR) mix (RCA-100-SBR). The latter was designed to achieve the same performance as concrete made with NA. Mixes were exposed to temperatures of 200 °C, 400 °C and 600 °C. After cooling, durability-loss due to thermal exposure was evaluated through water porosity, capillary water absorption, permeability, chloride diffusion and accelerated carbonation tests. At room temperature, the direct addition of RCA decreased all durability parameters. The SBR mix recovered some of the durability properties. Exposure to high temperatures decreases all the properties, but it varies depending on the property. The concrete made with NA and the SBR mix showed similar performance. The durability was also evaluated using a performance-based approach, both at

room and high-temperature. The proposed approaches showed potential to evaluate durability indicators, but they should be considered with precaution. Overall, concrete made with RCA reduces the durability of concrete, with or without heat damage, but this decrease can be reduced with proper mix optimization. These evaluations contribute to the post-heating durability of concrete structures made with RCA, which is fundamental to the post-fire assessment of concrete structures.

Acknowledgments. The authors would like to thank the support of Groupe Cassous (Guyenne Environnement and AQIO) and Groupe Garandeau.

Funding. This study was funded by Région Nouvelle-Aquitaine (project RECYFEU).

Conflict of interest. The authors declare that they have no conflicts of interest.

Availability of data and materials. All experimental data that support the findings of this study can be obtained from the corresponding author.

1 Introduction

The use of recycled coarse aggregate (RCA) as a replacement for natural aggregates has proven to be a possible solution to make sustainable concrete. This solution showed ~~potential to minimize~~ the potential to minimise the consumption of raw materials and also reduce waste ~~landfilling~~ landfill [1–3]. The production of recycled aggregate concrete (RAC) has been the aim of study for the last decades. In general, concrete made with RCA shows comparable properties to ordinary concrete, depending on RCA's quality and replacement rate [4, 5].

Although its use has been proven to be feasible, RCA will severely affect the properties of the concrete. First, related to the aggregate itself, RCA usually presents higher porosity, higher water absorption and lower strength than NA [2, 6] ~~,~~due to the attached (or adhered) mortar. Also, incorporating RCAs on concrete will result in a peculiar microstructure, with three different transition zones [2, 7]. These changes affect the behaviour of this sustainable concretes. ~~Extensive~~ In recent years, extensive research has been done ~~in the last years to characterize the RAC concrete~~ to characterise RAC behaviour. However, some topics still need to be addressed, primarily related to exposure to extreme conditions, such as fire and post-fire durability.

Indeed, these properties have been studied before in literature [8, 9], but limited attention was given to durability-loss due to exposure to elevated temperatures. Kou et al. [10] evaluated water absorption and porosity of RAC after exposure to elevated temperatures. The authors state that after exposure to 500 °C, water absorption was higher for concrete made with RCA, and this behaviour inverses after 800 °C. Mercury Intrusion Porosimetry (MIP) results demonstrated that the concrete with RCA presented a lesser increase in total porosity and smaller average pore diameter. The authors state that this behaviour is associated with better thermal compatibility between new and old paste.

Xuan et al. [11] also evaluated porosity through MIP and found RAC after 600 °C are more porous than concrete made with NA and carbonated RCA. They attributed this behaviour to the decomposition of hydration products from the cement mortar in RAC. Laneyrie et al. [12] evaluated the effect of high temperature on the water accessible porosity. They pointed out that water porosity did not change significantly up to 300 °C. Finally, Ma et al. [13, 14] evaluated the residual chloride permeability of RCA after exposure to high temperatures. They state that substituting NA with RCA ~~increased~~ increases the chloride diffusion coefficient, and this value increases as RCA content increases.

There is a lack of knowledge about the post-heating durability of concrete made with RCA. Several crucial parameters, such as permeability and carbonation ingress, were not evaluated after exposure to elevated temperatures. Moreover, even for ordinary concrete made with NA, the durability of fire-damaged concrete is little know and often ignored in standards and guidelines [15]. It is noteworthy that the post-heating durability should be assessed after

extreme events such as fire. Moreover, to be in use again, structures should meet the requirements of serviceability, strength and stability during ~~all~~ the remaining service life. The remaining durability properties should be assessed, and only after this evaluation ~~,~~ the strategies for repair, strengthening, and maintenance can be made.

To contribute to these knowledge gaps, this paper experimentally evaluates the residual durability of concrete made with RCA subjected to elevated temperature. Concretes made with NA and with 100 % of RCA were produced. For 100 % of substitution, a specific mix with comparable strength as concrete with NA was also designed. The mixes were heated to three different temperatures (200 °C, 400 °C and 600 °C). A comprehensive range of durability tests was done before and after exposure to high temperatures: water porosity, capillary water absorption, gas permeability, chloride diffusion and accelerated carbonation. Lastly, the concrete durability was evaluated using a performance-based approach.

2 Experimental program

2.1 Materials and concrete mixes

All materials were the same for the tested concretes except for coarse aggregate in this study. The cement was CEM II/A-L 42.5R (produced by Eqiom). The limestone filler was Betocarb HP-SC (produced by Omya). The superplasticizer was SIKA ViscoCrete Tempo-483. Alluvial sand was the fine aggregate chosen for the mixes. The two coarse aggregates were natural (NA) and recycled concrete aggregates (RCA). The NA was made from diorite, obtained from a quarry located in Genouillac (France). The ~~RCA~~ RCAs were crushed and screened near Bordeaux (France) by a recycling company. Table 1 ~~present~~ presents materials properties.

Table 1: Materials properties

Property	Cement	Filler	Sand	NA 4/10	NA 10/20	RCA 4/10	RCA 10/20
Density (kg/m^3)	3010	2700	2650	2820	2840	2570	2590
Specific surface (cm^2/g)	4700	4330	-	-	-	-	-
Water absorption (%)	-	-	0.35	0.92	0.81	5.6	4.52
LA coefficient (%)	-	-	-	16	16	30	36
Fineness modulus	-	-	3.1	-	-	-	-

Three concrete mixes were studied: concrete with NA (reference), 100 % direct replacement (DR) mix (RCA-100-DR) and 100 % strength-based replacement (SBR) mix (RCA-100-SBR). The concrete with NA was initially designed to meet durability requirements (NF EN 206/CN:2014 [16]) for the XD3 exposure class: water/cement (w/c) ratio of 0.5, C35/45 compressive strength class and cement content of 350 kg/m^3. This was done considering the most used concrete mix in the partner company. In RCA-100-DR, ~~NA~~

NAs were replaced by ~~RCA~~ RCAs in volume, without any changes in other constituents. In RCA-100-SBR, cement and water content were also adjusted to achieve the same strength and ~~slump~~ target slump (between 180 mm and 200 mm) as the reference mix. The SBR mix was designed with BetonLab [17] software. Based on compressive strength results of reference and DR mixes, aggregates properties were calibrated. Then, the w/c ratio was adjusted to have the same compressive strength as the reference. Finally, water and cement content were modified (maintaining the same w/c) to achieve the same slump. Table 2 ~~present mixture proportions. Compressive strength results of NA and DR mixes were used to calibrate the software's aggregate properties. Then, the w/c ratio and cement paste content were adjusted to achieve the same strength and workability as reference concrete. Table 2 present~~ presents the mixture proportions.

Working with wet aggregates instead of fully-saturated aggregates (soaked) was adopted~~thinking in~~ , thinking of a method that can be easily reproduced in the concrete plant from the partner company of the project. The aggregates (sand, NA and RCA) were pre-wetted for one hour using a soaker hose and then covered with a plastic sheet for three hours. The aggregates (sand, NA and RCA) were pre-wetted for one hour using a soaker hose and then covered with a plastic sheet for three hours. Before casting, moisture content was measured, and the ~~mix~~ mixing water was adjusted to reach the same slump. Additional water corrections were done due to variations in initial mixes. More details are given in previous works [18, 19].

The mixing procedure was the same for all mixes. First, aggregates, cement and filler were mixed for 2 minutes. Then, water and SP were added and mixed for two minutes. The slump was measured following NF EN 12350-2 [20]. Concrete with NA presented slump of 205 mm, RCA-100-DR was 208 mm and RCA-100-SBR was 174 mm. Cylindrical specimens of 11 cm x 22 cm and prisms of 7 cm x 7 cm x 28 cm were cast. The samples for mechanical characterization at 28 days were kept submerged in water at 20 °C. The remaining experimental samples were kept submerged for seven days and then placed into sealed plastic containers until test age: approximately 6 months for all tests, with the exception of carbonation samples, which aged 12 months. For concrete mechanical characterization, compressive strength (NF EN 12390-3 [21]), splitting tensile strength (NF EN 12390-6 [22]) and elastic modulus(NF EN 12390-13 [23]) were determined (Table 2).

2.2 Elevated temperature exposure

The heating process was done using an electric furnace of internal dimensions of 55 cm x 50 cm x 31 cm. The time-temperature parameters are controlled by an automated regulator connected to a thermocouple located inside the furnace. The furnace has electric resistance located in the back and a fan at the top to homogenize temperature properly. A low heating rate of 2 °C/min was chosen to avoid significant thermal gradients inside the concrete sample. Three temperatures were considered: 200 °C, 400 °C and 600 °C. ~~The~~ These

Table 2: Mix proportions and mechanical properties of studied mixes

Material/Property	Mix		
	NA	RCA-100-DR	RCA-100-SBR
Cement (kg/m^3)	350	350	420
Filler (kg/m^3)	60	60	60
Sand (kg/m^3)	804.3	804.3	799.8
NA 4/10 (kg/m^3)	331.7	-	-
NA 10/20 (kg/m^3)	711.1	-	-
RCA 4/10 (kg/m^3)	-	302.3	291.5
RCA 10/20 (kg/m^3)	-	648.5	630.3
Water (kg/m^3)	175	175	168
SP (% of cement)	0.9	0.9	0.9
f_{c28} (MPa)	42.2 (± 0.6)	32.6 (± 0.3)	44.4 (± 0.8)
f_{t28} (MPa)	4.0 (± 0.1)	3.8 (± 0.1)	4.0 (± 0.1)
E_{c28} (GPa)	32.9 (± 0.5)	27.1 (± 0.2)	30.1 (± 0.3)

temperatures were selected since the most relevant physicochemical changes occur within this temperature range. In addition, after 600 °C, most of the concrete strength has already gone [9]. The target temperature was kept for 180 min at the target temperature, then naturally cooled to room temperature inside the furnace. After cooling, samples were stored inside sealed containers with silica gel until testing.

2.3 Determination of durability procedures

2.3.1 Water accessible porosity

The water porosity was measured based on AFREM recommendations [24]. Three 1/4 of 11 cm x 5 cm disks, removed from the middle of cylinders, were used for each mix and temperature. For room temperature measurements, samples were oven-dried at 80 °C until constant mass (mass variation less than 0.05 % in one day) before testing. Eq. (1) presents the equation for water porosity (η, in %) calculation.

$$\eta = \left(\frac{m_{ssd} - m_{dry}}{m_{ssd} - m_{hyd}} \right) \cdot 100 \quad (1)$$

In these equations, m_{ssd} (kg) is the saturated superficially dried mass, m_{dry} (kg) is the dried mass, and m_{hyd} (kg) is the hydrostatic mass.

2.3.2 Gas permeability

Axial gas permeability was measured using the RILEM-CEMBUREAU method [25, 26], based on the Klinkenberg approach [27]. The test was carried out at room temperature and after each heating/cooling procedure described above. Three samples (⌀11 cm x 5 cm) per mix and temperature were evaluated. These disks were cut from ⌀11 cm x 22 cm cylinders using a diamond saw. The extremities (2 cm) of the ⌀11 cm x 22 cm cylinders were discarded to

avoid any possible edge effect on the permeability measurements. Before testing, samples were oven-dried at 80 °C. Then, the curved face of the cylinders was wrapped with aluminium tape to seal the sample, avoid any leakage and induce unidirectional flow.

The sample was placed in the permeameter cell, encased by a polyurethane ring and an inflated rubber tube. Once the sample was set, the rubber tube was inflated to apply lateral pressure on the specimen. The lateral pressure applied was 0.3 MPa, determined in trial tests with different confining pressures. These trial tests were done to verify the minimum value without any gas leakage on the setup. The reduction in lateral pressure was made based on Miah et al. [28], which showed that confining pressure strongly affects permeability measurements due to the closure of heat-induced microcracks. In any case, injected pressures were limited to half of the confining pressure.

The test principle consists of applying ~~a~~ an inert gas (nitrogen in this work) at constant pressure and, after stabilization, measuring the flow rate at the inlet. Three inlet gas pressure levels were used for each sample. For each pressure, the apparent permeability (K_a) was first determined according to Eq. (2) (based on Darcy's Law). The intrinsic permeability (K_{int}), which is independent of inlet pressure, was determined from the three apparent permeability measurements using the Klinkenberg correction for gas slippage [27]. For this, experimental data is fitted to ~~the~~ Eq. (3) to determine the intrinsic permeability of the material. Also, apparent permeability at 0.2 MPa, used for the performance-based approach (Section 4), was determined from the fitting.

$$K_a = \frac{2P_{atm}Q_iL\mu}{A({P_i}^2 - {P_{atm}}^2)} \tag{2}$$

$$K_a = K_{int}\left(1 + \frac{\beta}{P_m}\right) \tag{3}$$

In these equations, K_a (m^2) is the apparent permeability, K_{int} (m^2) is the intrinsic permeability, P_i (Pa) is the inlet pressure , P_{atm} (Pa) is the atmospheric pressure, Q_i (m^3/s) is the gas flow, L (m) is the sample thickness, μ (Pa/s) is dynamic viscosity of the inlet gas at the temperature measured during the test, A (m^2) is the cross-section sample area, and β (Pa) is the klinkenberg's coefficient.

2.3.3 Capillary water absorption

The capillary water absorption was measured based on AFREM recommendations [24]. From the 28 cm x 7 cm x 7 cm prisms, two samples of 14 cm x 7 cm x 7 cm (height x length x width) were obtained and used for each mix and each temperature level. The height of the specimen was chosen based on a previous work [29], which showed a high capillary rise of samples heated up to 600 °C. For room temperature measurements, samples were oven-dried at 80 °C before testing ~~,~~ until constant mass (mass variation less than 0.05 % in one day). The lateral surface (7 cm x 14 cm) were coated with epoxy resin to ensure one-dimensional water transport. After resin drying, one of the uncoated sides

(14 cm x 14 cm) was placed inside a covered recipient with water. Small metallic supports were used to provide 3 mm of immersed depth. The mass of each sample was measured at different time intervals (from 0.25 and up to 72 hours). Capillary water absorption was calculated using Eq. (4).

$$C_{wa} = \frac{m_t - m_0}{A} \tag{4}$$

Where C_{wa} (kg/m^2) is the capillary absorption, m_t (kg) is mass at time t, m_0 (kg) is initial mass and A (m^2) is the cross-section sample area in contact with water.

2.3.4 Chloride diffusion

The effective chloride diffusion coefficient was measured based on the accelerated migration test in steady-state conditions proposed by LMDC [30]. In this test, an electrical field is applied to a saturated concrete specimen placed between two compartments, upstream (a solution rich in chlorides) and downstream (a solution without chlorides). The chloride diffusion coefficient is determined from the chloride ion flux between compartments [30–32]. For this, concrete disks of ⌀11 cm x 5 cm were sawn from ⌀11 cm x 22 cm cylinders. Two samples per mix and temperature were evaluated. Measurements were limited to 200 °C ~~,~~ since the crack state of samples after 400°C did not ~~allowedproper~~ allow proper determination of the chloride coefficient with the proposed method.

After vacuum saturation with a support solution (demineralised water, 1 g/l of $NaOH$, and 4.65 g/l of KOH), samples were placed in the migration cell. A constant potential of 30 V was applied between the electrodes to provide an electric field (E = 600 V/m) between downstream and upstream compartments. The upstream compartment contained a solution of $NaCl$ (12 g/l), $NaOH$ (1 g/l), KOH (4.65 g/l) and demineralised water, while the downstream compartment was filled with the ~~the~~ support solution. The concentration of chloride ions in the upstream was determined by $AgNO_3$ titration. This measurement was done before the start of the test and at regular intervals: two times per day for five days. For the calculation, first, the ionic flux of chlorides (J, in mol/m^{3}s) was determined using the slope of the curve of the variation between the cumulative quantity of chlorides leaving the upstream versus time, as shown in Eq. (5). Then, the effective chloride diffusion coefficient (D_{eff}, in m^2/s) was calculated, following Eq. (6).

$$J = \frac{C_{up,1} - C_{up,2}}{t} \cdot \frac{V}{S} \tag{5}$$

$$D_{eff} = \frac{RTJ}{C_{up}FE} \tag{6}$$

Where $C_{up,1}$ and $C_{up,1}$ (mol/m^3) are the concentration of chlorides at upstream in the start and at the moment of the test, t (s) is test duration, V (m^3) is the volume of the upstream solution, S (m^2) is the surface area of test

specimen exposed to chloride, R (8.314 J/molK) is the perfect gas constant, T (K) is the temperature during chloride test, C_{up} (mol/m^3) is chloride concentration of the upstream solution, F (96 487 C/mol) is Faraday constant and E (V/m) is the electric field applied.

2.3.5 Accelerated carbonation

The carbonation was evaluated by accelerated testing. The test protocol was based on French Standard XP P18-458 [33], with some differences described below. Concrete disks of ⌀11 cm x 6.5 cm were sawn from ⌀11 cm x 22 cm cylinders using a diamond saw. The pre-conditioning involved different steps. First, samples were dried in a ventilated oven at 45 °C for 14 days. Then, samples were placed in a climatic chamber at 20 °C and 65 % HR for 14 days. For heated samples, the pre-conditioning involved an additional step. Since they were fully dried after heating, samples were immersed in water for 48 hours. This process was done to re-saturate the sample and recover the necessary humidity (usually between 50 % and 80 % [34]) for the carbonation phenomenon. Then, samples underwent the same procedure described before (drying for 14 days followed by 14 days inside the climatic chamber). Just before the test, the curved face of each cylinder was wrapped with aluminium tape to ensure a unidirectional carbonation flow.

The samples were then placed inside the carbonation chamber with 3±0.5 % of CO_2, relative humidity of 65±5 % and temperature of 20±3 °C. It is noteworthy that the CO_2 content used was much lower than the 50 % specified in the XP P18-458 [33] standard. The value was chosen based on previous studies, which showed that 3 % is suitable and representative of long-term carbonation in natural conditions [35, 36]. After 0, 2, 7, 14, 21 and 28 days of exposure, one disk per mix and temperature was removed and split into two parts through splitting tests. Phenolphthalein was sprayed ~~in the fractures~~ on the fractured surfaces, and carbonation depth was measured using a ~~calliper~~caliper. Five depth measurements were taken from each side (top/bottom) of each part, and, in total, 20 values were taken per mix/condition. In addition to carbonation depth, the carbonation rate was calculated using Eq. (7), based on square root theory and in accord with the second law of Fick [37].

$$X_c = k_{acc}\sqrt{t} \tag{7}$$

Where X_c (mm) is the carbonation depth, k_{acc} (mm/yr$^{1/2}$) is accelerated carbonation rate and t (yr) is time.

3 Results

3.1 Water accessible porosity

The evolution of water porosity with temperature is presented in absolute (Fig. 1a) and relative values (Fig. 1b). First, at room temperature, concrete with NA showed a porosity of 11.4 %, and the direct substitution of coarse NA by RCA

resulted in a porosity increase to 16.2 %. The results and ~~as well the increase~~ the rise in water porosity are coherent with previous works [38]. For the SBR mix, the porosity remains close to the DR mix, 15.7 %. This behaviour shows that water porosity, in the case of concrete made with RCA, is mainly driven by RCA porosity.

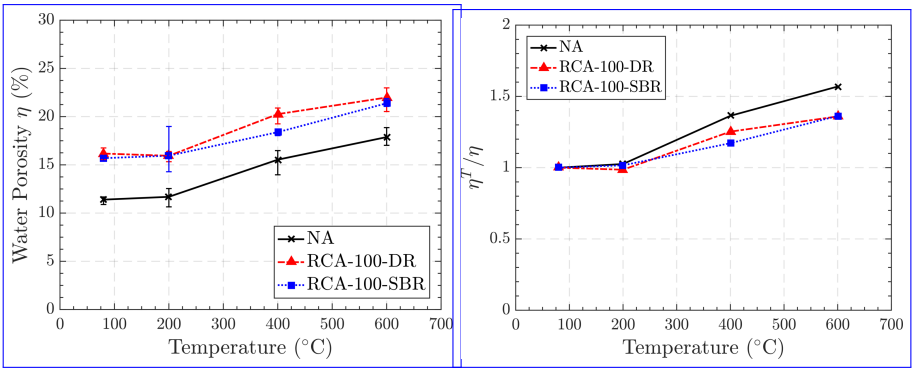

(a) absolute values (b) relative values

Fig. 1: Evolution of water porosity with temperature

The evolution of water accessible porosity with temperature was similar for all tested concrete (Fig. 1a). First, up to 200 °C, the porosity almost did not change for studied mixes. Similar behaviour has been registered in previous works that studied NA ~~,~~ and RCA concretes [12, 39]. From 200 °C to 400 °C, the porosity starts to increase significantly, and it is mainly related to intense water loss and decomposition of C-S-H [40]. In the last branch, from 400 °C to 600 °C, water porosity increases again at a higher rate and is mainly associated with portlandite decomposition.

In general, concrete with NA presents the lowest water porosity values for all tested temperatures. The difference between NA and RCA is close to 3 % and 4 % at all temperatures. Both RCA mixes (DR and SBR) show similar values, ~~except~~ except for 400°C ~~, when~~ when the difference reaches 1.8 %. This behaviour highlights again that aggregate plays a crucial role in ~~the~~ water accessible porosity. Reducing w/c and increasing the cement paste did not change the water porosity significantly. In terms of relative porosity evolution, concrete with NA presented higher values than the mixes with RCA. This higher rate is probably related to the higher thermal mismatch in the NA mix that promotes microcracks. The evolution observed in concrete made with RCA is lower, probably due to the better match between new cement paste and old cement paste.

3.2 Gas permeability

Gas permeability results are presented in Fig. 2a and 2b. For room temperature (first points on Fig. 2a), the direct addition of coarse RCA appears to increase the gas permeability, as observed in previous works [38, 41]. However, contrary to the phenomenon observed in the water porosity, the strength-based replacement mix shows intrinsic permeability closer to concrete with NA. This result ~~shows~~ indicates that the cement matrix plays a key role in permeability. It is noteworthy also that the changes in permeability were observed within the same exponent (around 10^{-16}); hence, care should be taken when interpreting the results. In any case, similar findings were observed in previous studies [38, 42] that verified that the difference between k_{int} in concrete with NA and RCA is lower when the matrix quality is improved.

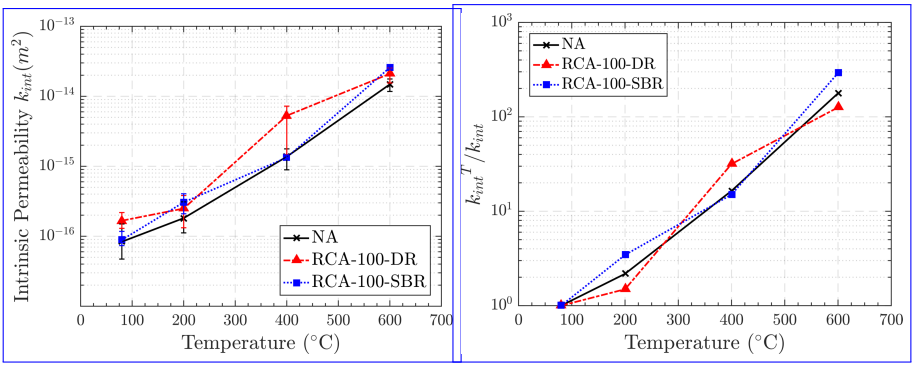

(a) absolute values (b) relative values

Fig. 2: Evolution of permeability with temperature

Fig. 2a presents the evolution of permeability (absolute values in log scale) with all tested temperatures. Concrete with NA presented lower permeability for any given temperature, again highlighting the primary effect of initial aggregate properties. Both DR and SBR ~~shows~~ show differential behaviour depending on the temperature level. At 200 °C, SBR and DR permeability were almost the same. This behaviour can be associated with ~~the~~ cracking and porosity due to water evaporation in cement paste. However, at 400 °C, the DR mix is almost four times more permeable than SBR, even though dispersion is high. Given that RCA porosity is the same, a probable reason is related to the cracking at cement paste and interfaces. The stronger cement paste in the SBR mix possibly reduces general cracking in the paste and reduces thermal mismatch between RCA and paste. At 600 °C, values approach again, with both mixes having similar behaviour.

Fig. 2b presents the evolution of permeability relative values (in log scale) with temperature. The same variation observed in absolute is also shown in relative values: concrete with NA presents a steady growth in permeability, while DR and SBR mix varies depending on temperature. The graph reveals the significant increase in DR permeability between 200 °C and 400 °C, highlighting the probable damage of cement paste and interface at this temperature level. Finally, from 400 °C to 600 °C, the growth is higher in the SBR mix, probably related to the degradation in portlandite and sand quartz transformation at this temperature level [40].

3.3 Capillary water absorption

The effect of RCA on the capillary water absorption is presented in Fig. 3a. This figure illustrates the evolution of water absorption with the square root of time (each curve is the average of two samples) for samples at room temperature. The RCA-100-DR presents higher absorption than the other two mixes at any given time. This behaviour is the same as reported in previous works and directly linked to the higher absorption and porosity of RCA [41, 43]. In the SBR mix, the changes in w/c and cement paste decreases the capillary water absorption curves: they get closer to what is observed in concrete made with NA. This improvement ~~isrelated~~ is related to the improvement in the cement matrix of RCA-100-SBR, which presents higher compacity than RCA-100-DR.

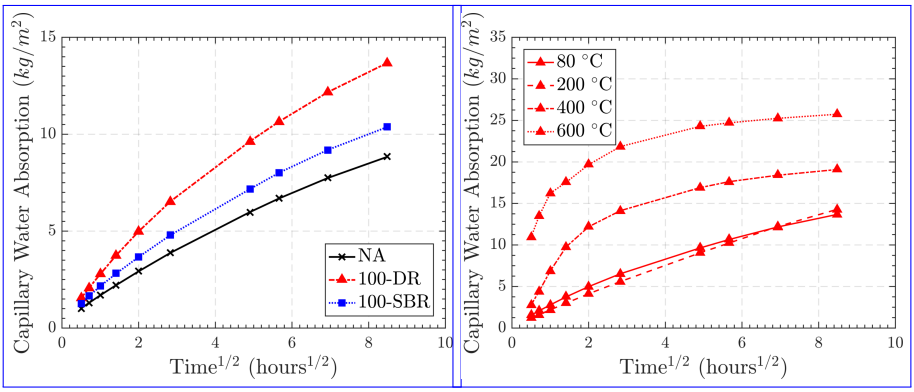

(a) room temperature (b) elevated temperatures (RCA-100-DR)

Fig. 3: Evolution of capillary water absorption with time

The evolution of capillary water absorption with the square root of time varies significantly depending on the temperature level (an example is given ~~at~~ in Fig. 3b). Up to 200 °C, the behaviour is quite linear, as seen in typical absorption curves. However, from 400 °C to 600 °C, the curves present a different evolution, with two distinct phases: a first one, with a higher absorption rate, followed by a flattened phase. The behaviour is similar to what was

observed in previous works [44, 45], which evaluated the effect of damage on absorption. The cracks act as a preferential flow and provide access to air-filled pores, usually filled only later in un-damaged concrete. In the second phase, with the lower rate, the air-filled voids had already been filled, explaining the behaviour in this second period. Given this behaviour, to ~~analyze~~ analyse the results with temperature, it was chosen to evaluate the water absorbed at 72 hours as the primary indicator.

Fig. 4a presents the evolution of 72-hour capillary water absorption versus temperature. From room to 200 °C, the absorption was almost constant for all mixes, showing that the crack state is not relevant to induce higher absorption at this temperature. From 200 °C to 600 °C, a linear increase is observed, and it is due to crack development and dehydration. In general, concrete with RCA presented higher absorption than concrete made with NA. The same behaviour was verified in Kou et al. [10]. This behaviour is mainly attributed to RCA's higher porosity and mortar content, which drive the capillary water rise in these concretes. The SBR mix presented lower values than DR, showing that paste improvement reduced the capillary pores. If the RCA-100-DR presented higher absolute values, this mix presented a lower evolution (Fig. 4) in terms of relative values. NA and RCA-100-SBR showed close growth. The highest evolution of concrete made with NA could be related to the worst thermal mismatch in this type of concrete. However, this is not the case ~~of~~ for RCA-100-SBR, which presents an equal mismatch as RCA-100-DR. In this case, the evolution can be related to the higher deterioration of hydration products of cement paste as temperature increases.

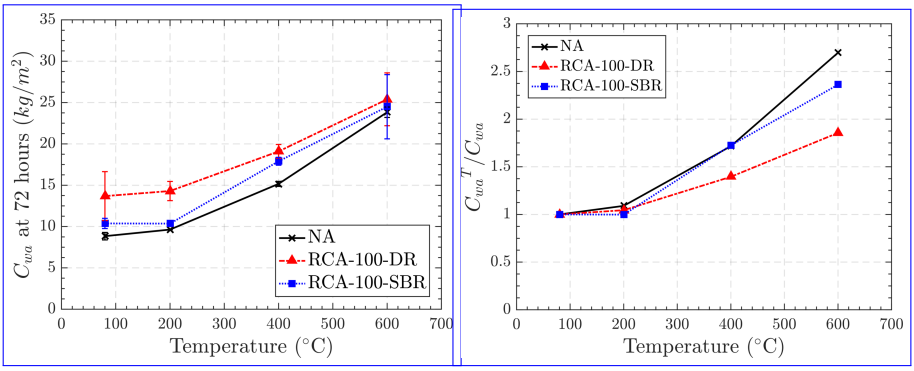

(a) absolute values (b) relative values

Fig. 4: Evolution of capillary water absorption with temperature

3.4 Chloride diffusion

Fig. 5 presents the evolution of chloride diffusion coefficient (in log scale) with temperature. At room temperature, the direct addition of RCA increases almost by seven the chloride diffusion coefficient. The lower resistance of RAC to chloride penetration has been verified in previous works [38, 43, 46]. It is noteworthy that RCA-100-DR presented a relevant variation in measurements (relevant error bar), but the mix presented higher diffusion than NA in all samples. The increase in chloride diffusion for SBR was lower than in the DR mix, but the average value did not return to the reference concrete level. Indeed, the chloride evolution behaves similarly to water porosity behaviour: the reduction of w/c and increase in cement paste did not overcome the higher RCA porosity. The influence of RCA porosity on chloride behaviour is also reported in some previous work [46, 47].

For high temperature evolution, as explained in the methodology, the coefficient was not possible to measure after 200 °C ~~,~~ due to the crack state of the samples. In any case, it is seen that concrete with NA presents the lowest chloride diffusion for the two tested temperatures. However, the difference between concrete with NA and RCA ~~mixes is lower than~~ is lower at 200 °C. From room temperature to 200 °C, both NA and RCA-100-SBR increased significantly, probably due to the development of microcracks in the material. It is noteworthy that the evolution in RCA-100-DR is much lower than in the other mixes. This is coherent with permeability and porosity evolution, which was lower for RCA-100-DR. The worst behaviour in concrete made with RCA for chloride was also reported in Ma et al. [13]. They verified that increase in RCA content increased the chloride permeability.

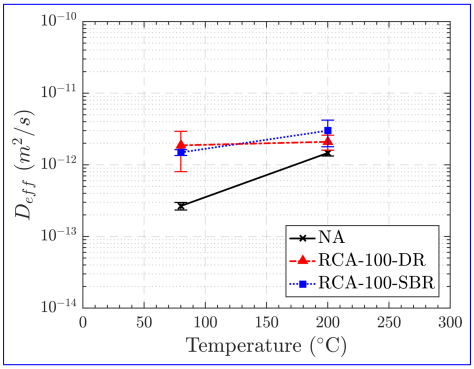

Fig. 5: Evolution of chloride diffusion coefficient with temperatures

3.5 Accelerated carbonation

Table 3 presents an overview of all the results from accelerated carbonation tests. The carbonation rate was calculated using Fick Law's and each graph of

carbonation depth versus test duration. The high r^2 of the regression curves shows that this model is appropriate even for the case of high-temperature exposure.

Table 3: Carbonation results after exposure to elevated temperature (average values and standard deviation)

Mix	Parameters	Temperature			
		23°C	200°C	400°C	600°C
NA	Depth at 28 days (mm)	6.42 (1.02)	8.04 (1.08)	9.84 (0.89)	12.20 (1.21)
	Carbonation rate (mm/yr$^{1/2}$)	1.14	1.49	1.79	2.51
	r^2	0.93	0.97	0.97	0.97
RCA-100-DR	Depth at 28 days (mm)	10.37 (1.85)	11.49 (0.85)	11.62 (0.81)	20.49 (1.66)
	Carbonation rate (mm/yr$^{1/2}$)	1.93	2.15	2.29	3.72
	r^2	0.99	0.98	0.97	0.98
RCA-100-SBR	Depth at 28 days (mm)	6.24 (0.93)	6.76 (0.81)	8.90 (0.87)	13.87 (2.16)
	Carbonation rate (mm/yr$^{1/2}$)	1.14	1.32	1.77	2.69
	r^2	0.96	0.97	0.95	0.97

For room temperature, the carbonation depth at 28 days of RCA-100-DR was 1.6 times greater than the reference mix. This is coherent with previous works [48], which verified that relative carbonation depth increases with RCA due to higher porosity and absorption of RCA aggregates. Silva et al. [48], with a statistical approach in a literature compilation, showed that RCA usually presents a carbonation depth 2.5 times higher than ordinary concrete. The adjustment of cement paste in the SBR mix improved the carbonation resistance of RAC mixes, and the depth was even slightly lower than concrete with NA. This behaviour is also verified in previous works, which adjusted the w/c ratio to obtain the same target strength [48, 49]. The same behaviour was identified using the accelerated carbonation rate. The evolution was equal for NA and RCA-100-SBR, highlighting that improving cement paste can result in similar carbonation performance.

To compare the effect of temperature in each mix, carbonation rate versus temperature was plotted in Fig. 6. Fig. 6a presents the evolution of carbonation rate with temperature in absolute values. The behaviour seen ~~in~~ at room temperature keeps similar for all tested temperatures. The direct addition of RCA increased the carbonation rate, while the SBR mix showed similar performance to concrete made with NA. After exposure to 600 °C, the rate in RCA-100-DR was almost 1.5 more elevated than in concrete made with NA. The difference in carbonation depth after 28 days was more than 8 cm higher, as seen in Table 3. The same table and figure show that concrete made with NA and RCA-100-SBR presented minor differences in rate and carbonation depth. This indicates that the paste enhancement for SBR was also helpful for carbonation performance.

For absolute values, the evolution of carbonation rate with temperature is quite similar in all studied mixes. From 23 °C to 400 °C, the evolution rate was relatively low, especially for RCA-100-DR. In this case, the carbonation rate varied from only 0.36 mm/yr$^{1/2}$. At this temperature, the changes are related

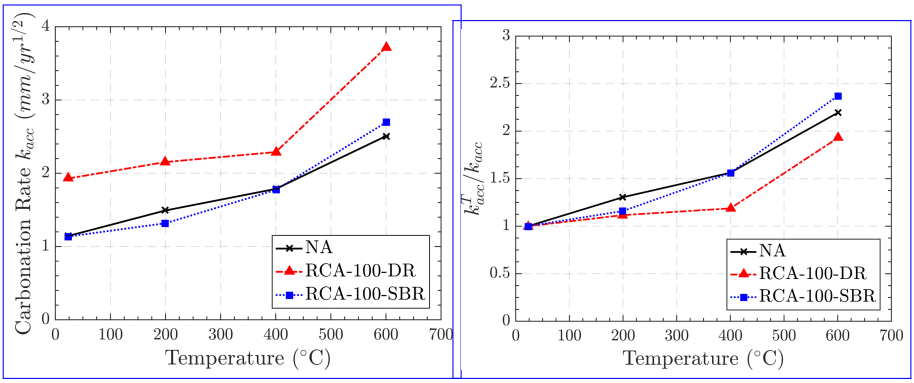

(a) absolute values (b) relative values

Fig. 6: Evolution of carbonation rate with temperature

to the increase of porosity and permeability due to water loss and first C-S-H dehydration. From 400 °C to 600 °C, the increase in carbonation rate was substantial. At 600 °C, concrete suffers from deterioration due to portlandite dehydration and thermal mismatch. When analyzing the relative values (Fig. 6b), a similar behaviour to the other indicators is observed. Concrete with NA and RCA-100-SBR presents higher evolution. And, even though the increase from 400 °C to 600 °C is relevant, the growth in RCA-100-DR is lower than the other two.

4 Towards a performance-based approach

Different analyses were proposed to evaluate the durability performance of concrete made with RCA. They were divided into two sections concerning temperature exposure: at room temperature and after elevated temperatures. In the first case, the objective was to evaluate the effect of replacement rate on concrete durability. The second case refers to the effect of temperature on concrete durability.

Two different performance-based approaches were proposed at room temperature to evaluate the durability of concrete made with RCA. The first is the equivalent performance concept, based on NF EN 206-1/CN:2014 [16] prescription. In this method, the new concrete should have an equal or better performance than the concrete designed according to the durability requirements from NF EN 206-1/CN:2014 [16]. In this project, ~~both~~ RCA-100-DR and RCA-100-SBR are compared to the concrete made with NA. An index of equivalent performance (EP^R) was calculated for each property. These indexes are the ratio between the property of concrete made with NA (X_{NA}) and concrete made with RCA (X_{RCA}). If the ratio is lower than 1, the concrete has deteriorated. If it is higher or equal to 1, concrete has improved or kept the performance of the reference. For permeability and chloride diffusion, the

index was calculated using the log values, and the final value was inversed to ~~compatibilize~~ match with the proposed scale. Eqs. (8) and (9) shows the index calculation. All values were plotted in a spider-plot type of graph (Fig. 7a). Similar approaches were made in previous studies [50–53].

$$EP^R{}_i = \frac{X_{NA}}{X_{RCA}} \tag{8}$$

$$EP^R{}_i = \frac{1}{\frac{\log X_{RCA}}{\log X_{NA}}} \tag{9}$$

In these equations, $EP^R{}_i$ is the equivalent performance index for the replacement rate. The index i varies from 1 to 5, where 1 is water porosity, 2 is intrinsic permeability, 3 is chloride diffusion coefficient, 4 is accelerated carbonation rate, and 5 is capillary water absorption at ~~72-hours~~72 hours.

The second approach for room temperature evaluation was the analysis based on the potential durability established by the AFGC guide for durability [54]. Selected (water porosity, permeability and chloride) were used to classify the concrete according to five classes: very low (VL), low (L), medium (M), high (H) and very high (VH). Table 4 presents the limits associated with each one of the evaluated properties. ~~To~~ For a comparative analysis, the values were normalized from 0 to 1, using Eq. 10. The 0 was defined as the very low limit (X_{vl}). It was chosen a value lower than the threshold presented in the table (18 for water porosity~~:~~ , 30 for chloride and 3000 for permeability). The 1 was the very high limit (X_{vh}) indicated in the table (in the case of water porosity, 9 was the adopted as threshold value). It is noteworthy that gas permeability and chloride diffusion were ~~calculated also~~ also calculated using base-ten logarithms. Using Eq. (10) and Table 4, the scale presented in Fig. 7b was proposed. In this figure, all the potential durability zones are indicated. Eq. (10) was also used to calculate the potential durability indicator for each of the studied mixes.

$$DI^R{}_i = \frac{X_i - X_{vl}}{X_{vh} - X_{vl}} \tag{10}$$

In these equations, $DI^R{}_i$ is the potential durability ~~indicators~~ indicator for each mix. The index i varies from 1 to 3, where 1 is water porosity, 2 is gas permeability at $P_i = 0.2$ MPa, and 3 is chloride diffusion coefficient. The X_i ~~correspond~~ corresponds to the property to be ~~normalized~~normalised, X_{vl} is the very low limit and X_{vh} is the very high limit.

For concrete after exposure to elevated temperatures, similar approaches were applied, but they were adapted considering the objective of the analysis. For the first approach, an equivalent concept was also proposed. But this time, the equivalence of each heated concrete was compared with its respective value at room temperature. In a post-fire scenario, the interest is in how much ~~from~~ of the initial durability remains. Hence, an index of equivalent performance at high temperature (EP^T) was calculated for each property. In this case, these

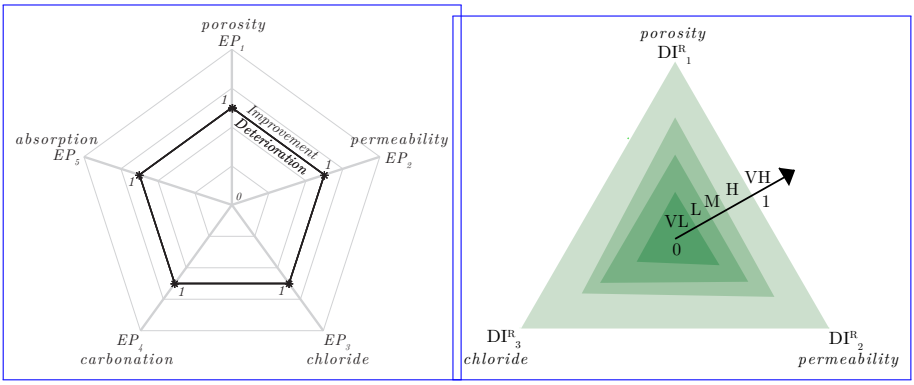

(a) Equivalent Performance (b) Potential Durability

Fig. 7: Scale used in performance approaches

Table 4: Durability indicators (adapted from [54])

Property	Classes and limit values				
	Very Low	Low	Medium	High	Very High
Water Porosity η (%)	>16	14 to 16	12 to 14	9 to 12	9 to 6
Effective chloride coefficient D_{eff} ($10^{-12}m^2/s$)	>8	2 to 8	1 to 2	0.1 to 1	<0.1
Gas permeability at ($P_i = 0.2$ MPa) k_{gaz} ($10^{-18}m^2$)	>1000	300 to 10000	100 to 300	10 to 100	<10
Compressive strength class (indicative)	-	C25 to C40	C30 to C60	C55 to C80	>C80

indexes are the ratio between the property of concrete at room temperature and concrete at high ~~temperature~~temperatures. The same principle of deterioration and improvement is applied. Since the chloride diffusion coefficient was determined only up to 200 °C, the analysis was done only in the four remaining parameters.

The potential durability approach following AFGC criteria was also applied for high-temperature evaluation. The method, including limits and ~~normalization~~ normalisation procedure, was the same as that used at room temperature. Since the chloride diffusion coefficient was determined only up to 200 °C, the analysis was done this time considering room temperature and 200 °C.

4.1 Room temperature

Fig. 8 presents the equivalent performance for the three studied mixes. When ~~analyzing~~ analysing the DR mix, it can be seen that the substitution of NA with RCA worsened all durability indicators. An improvement in ~~the~~ durability was achieved when ~~optimizing~~ optimising the w/c and the cement paste content to obtain the same strength as reference concrete. Even though the water porosity remains high, due to the high porosity of the RCA, the RCA-100-SBR

showed reduced deterioration in some indicators. This is especially highlighted for the accelerated carbonation rate. These results also highlight that water accessible porosity may not be the most appropriate indicator to evaluate durability.

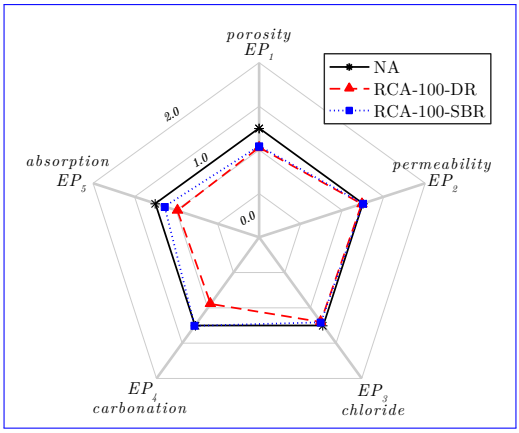

Fig. 8: Equivalent performance for mixes at room temperature

Fig. 9 presents the potential durability evaluation for the three studied mixes. Concrete with NA had different ~~potential~~ potentials according to the different parameters. Water porosity and chloride ~~indicates~~ indicate that the mix has high (H) durability, while permeability indicates that concrete has medium (M) durability. As the case of the equivalent comparison, the DR mix worsened all the performances. Water porosity and permeability were classified as very low (VL), and chloride showed medium potential durability. For the SBR mix, even though it has improved from the DR mix, this mix did not recover the same potential as the concrete made with NA. Gas permeability and chloride diffusion presented the same potential (medium). Still, water porosity was classified as low (L). It's noteworthy that, in this document, carbonation was not defined as a parameter for potential durability ~~indicator~~indicators. Hence, if only this approach were used, the improvement in carbonation resistance would not be verified. This highlights the necessity of precaution when evaluating durability through a similar approach.

4.2 Elevated temperatures exposure

Fig. 10 presents the equivalent performance analysis for exposure to elevated temperatures. A different mix is evaluated in each plot, and a curve for each temperature level is presented. For all mixes, it is seen that up to 200 °C, the performance is close to the room temperature. This shows that the concrete can retain some initial durability if heated only up to this temperature level. After 400 °C, the deterioration gets high, and the increase is more prominent in

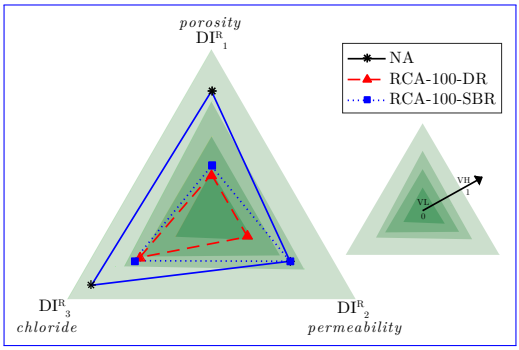

Fig. 9: Potential durability for mixes at room temperature

concrete with NA and RCA-100-SBR. This indicates that these mixes undergo higher damage up to this temperature, mainly associated with cracks due to water loss and paste hydrates deterioration. The lower evolution of RCA-100-DR can also be associated with the fact that the initial durability of this concrete is lower. Hence, the transformations at this level do not deteriorate indicators as much as the other mixes.

Fig. 11 presents the potential durability evaluation for the mixes after exposure to 200 °C. A similar trend ~~observed~~ in equivalent durability is also verified here: the RCA-100-DR degrades less than the other mixes. However, concrete with NA presents a better performance, even after exposure to high temperatures. The porosity keeps in the high zone potential, but permeability and chloride degrade one class: permeability ~~enter~~ enters to low durability zone, and chloride enters the medium durability zone. This behaviour reinforces that this concrete can retain some of its durability properties and may still be functional after exposure to this level. For RCA-100-DR, the values kept almost the same after exposure to 200 °C. However, it's noteworthy that the durability of this mix is already low at room temperature. Lastly, for RCA-100-SBR, porosity and chloride kept similar, with both staying in the same potential after exposure to 200 °C (low and medium, respectively). However, the permeability moved from medium to low potential, indicating a reduction in the performance of this concrete. In general, this methodology seems a good approach for evaluating post-fire durability.

5 Conclusions

This paper presented an experimental investigation into the post-heating durability of concrete made with recycled concrete aggregates. Based on the results, the following conclusions have been drawn:

- The direct addition of RCA in DR mixes reduced the durability of ordinary strength concrete. The reduction was prominent on all durability indicators. The reduction of w/c and increase in cement paste in the SBR mix

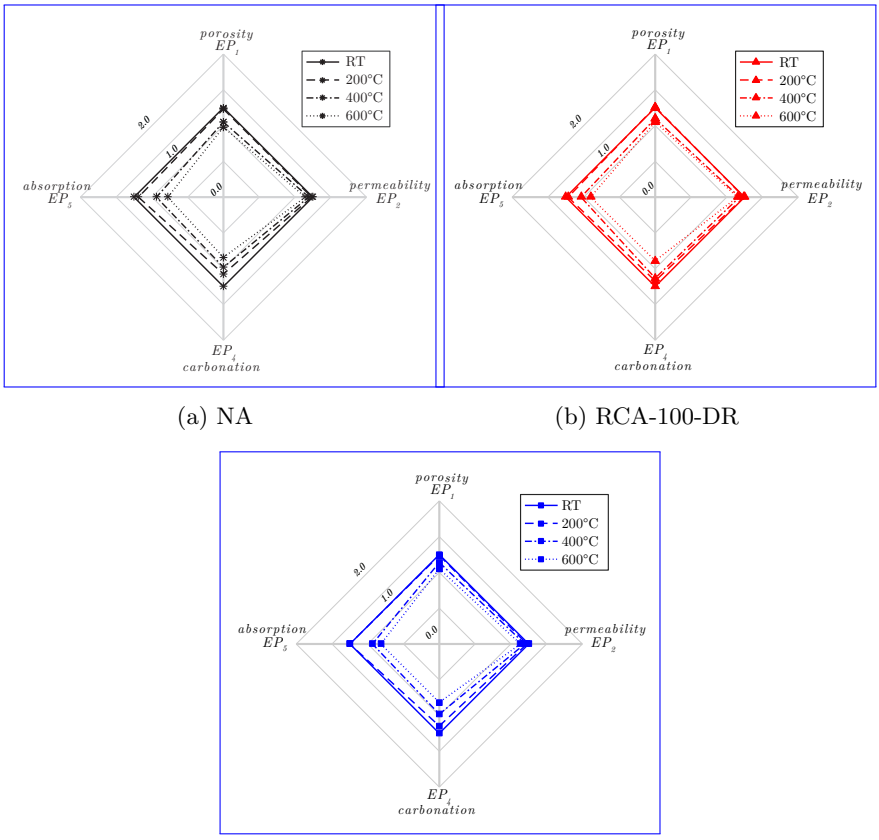

(a) NA

(b) RCA-100-DR

(c) RCA-100-SBR

Fig. 10: Equivalent performance for mixes at after exposure to high temperature

contributed to the recovery of some durability parameters. Even though water porosity ~~kept~~ was high for SBR mix, permeability and accelerated carbonation showed the same performance as reference concrete. The chloride diffusion coefficient and capillary water absorption were better than DR but not at the same level as concrete with NA. This behaviour highlights that the same compressive strength is not enough to guarantee the ~~exact~~ same durability, and these parameters should be evaluated.

- Exposure to high temperatures deteriorated the durability of all studied mixes, and the extent is greater as temperature increases. In general, the relative increase is lower for the DR mix and similar in the case of the NA and SBR mix. Capillary water absorption and water porosity evolved similarly, with almost constant values up to 200 °C, followed by a significant increase at 400 °C and 600 °C. Accelerate carbonation rate increased in a low rate up

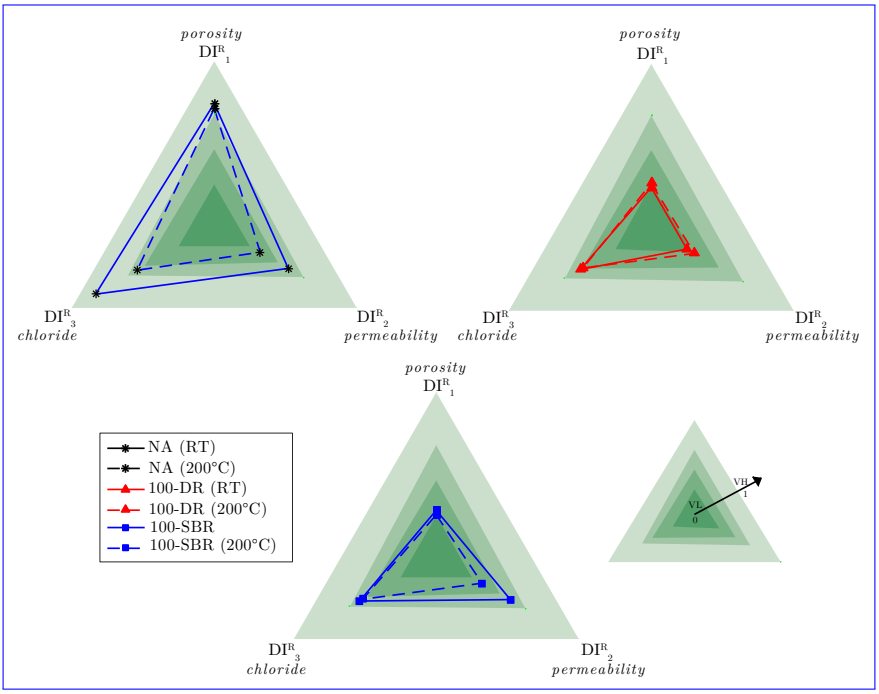

Fig. 11: Potential durability for mixes after exposure to elevated temperatures

to 400 °C, then a remarkable increase was observed after exposure to 600 °C. Permeability showed a different behaviour depending on the temperature level - with slight variations between all mixes. For chloride, NA presented lower values than RCA mixes, but the increase was higher.

- The proposed performance-based approaches showed potential to evaluate durability indicators. The equivalent performance concept showed potential, but some indicators (e.g. water porosity) should be considered with precaution. The potential durability concept was an excellent method to evaluate ~~the~~ durability, including the high-temperature scenario. However, this method should be updated and extended for different indicators (accelerated carbonation, for example).
- This paper shows that the addition of RCA reduces the ambient and post-fire durability of concrete made with RCA. However, with proper mix ~~optimization~~optimisation, the durability can be recovered to some extent.

References

[1] de Brito, J., Saikia, N.: Recycled Aggregate in Concrete, p. 448. Springer, London (2013). https://doi.org/10.1007/978-1-4471-4540-0. http://link.springer.com/10.1007/978-1-4471-4540-0

[2] Shi, C., Li, Y., Zhang, J., Li, W., Chong, L., Xie, Z.: Performance enhancement of recycled concrete aggregate - A review. Journal of Cleaner Production **112**, 466–472 (2016). https://doi.org/10.1016/j.jclepro.2015.08.057

[3] Nedeljković, M., Visser, J., Šavija, B., Valcke, S., Schlangen, E.: Use of fine recycled concrete aggregates in concrete: A critical review. Journal of Building Engineering **38**, 102196 (2021). https://doi.org/10.1016/j.jobe.2021.102196

[4] Le, H.-b., Bui, Q.-b.: Recycled aggregate concretes – A state-of-the-art from the microstructure to the structural performance. Construction and Building Materials **257**, 119522 (2020). https://doi.org/10.1016/j.conbuildmat.2020.119522

[5] de Larrard, F., Colina, H.: Conclusion. In: de Larrad, F., Colina, H. (eds.) Concrete Recycling: Research and Practice, pp. 544–545. CRC Press, Boca Raton (2019)

[6] Behera, M., Bhattacharyya, S.K., Minocha, A.K., Deoliya, R., Maiti, S.: Recycled aggregate from C&D waste & its use in concrete - A breakthrough towards sustainability in construction sector: A review. Construction and Building Materials **68**, 501–516 (2014). https://doi.org/10.1016/j.conbuildmat.2014.07.003

[7] Wang, R., Yu, N., Li, Y.: Methods for improving the microstructure of recycled concrete aggregate : A review. Construction and Building Materials **242**, 118164 (2020). https://doi.org/10.1016/j.conbuildmat.2020.118164

[8] Guo, H., Shi, C., Guan, X., Zhu, J., Ding, Y., Ling, T.C., Zhang, H., Wang, Y.: Durability of recycled aggregate concrete – A review. Cement and Concrete Composites **89**, 251–259 (2018). https://doi.org/10.1016/j.cemconcomp.2018.03.008

[9] Fernandes, B., Carré, H., Mindeguia, J.-C., Perlot, C., La Borderie, C.: Effect of elevated temperatures on concrete made with recycled concrete aggregates-an overview. Journal of Building Engineering, 103235 (2021). https://doi.org/10.1016/j.jobe.2021.103235

[10] Kou, S.C., Poon, C.S., Etxeberria, M.: Residue strength, water absorption and pore size distributions of recycled aggregate concrete after exposure to elevated temperatures. Cement and Concrete Composites **53**, 73–82 (2014). https://doi.org/10.1016/j.cemconcomp.2014.06.001

[11] Xuan, D., Zhan, B., Poon, C.S.: Thermal and residual mechanical profile

of recycled aggregate concrete prepared with carbonated concrete aggregates after exposure to elevated temperatures. Fire and Materials **42**(1), 134–142 (2017). https://doi.org/10.1002/fam.2465

[12] Laneyrie, C., Beaucour, A.-L., Green, M.F., Hebert, R.L., Ledesert, B., Noumowe, A.: Influence of recycled coarse aggregates on normal and high performance concrete subjected to elevated temperatures. Construction and Building Materials **111**, 368–378 (2016). https://doi.org/10.1016/j.conbuildmat.2016.02.056

[13] Ma, Z., Ba, G., Duan, Z.: Effects of high temperature and cooling pattern on the chloride permeability of concrete. Advances in Civil Engineering **2019** (2019). https://doi.org/10.1155/2019/2465940

[14] Ma, Z., Liu, M., Tang, Q., Liang, C., Duan, Z.: Chloride permeability of recycled aggregate concrete under the coupling effect of freezing-thawing, elevated temperature or mechanical damage. Construction and Building Materials **237**, 117648 (2020). https://doi.org/10.1016/j.conbuildmat.2019.117648

[15] Valente Monteiro, A., Vieira, M.: Effect of elevated temperatures on the residual durability-related performance of concrete. Materials and Structures/Materiaux et Constructions **54**(6), 13–15 (2021). https://doi.org/10.1617/s11527-021-01824-5

[16] Comité Européen de Normalisation: NF EN 206/CN: Béton — Spécification, Performance, Production et Conformité — Complément National à la Norme NF EN 206. Brussels (2014). Comité Européen de Normalisation

[17] de Larrard, F., Sedran, T.: BetonLab (2021). https://betonlabpro.ifsttar.fr/

[18] Fernandes, B., Carré, H., Mindeguia, J.-C., Perlot, C., La Borderie, C.: Spalling behaviour of concrete made with recycled concrete aggregates. Construction and Building Materials **344**, 128124 (2022). https://doi.org/10.1016/j.conbuildmat.2022.128124

[19] Fernandes, B.: Fire behaviour, spalling and residual durability of concrete made with recycled concrete aggregates. PhD thesis, Université de Pau et des Pays de l'Adour (2022)

[20] Comité Européen de Normalisation: NF EN 12350-2: Testing Fresh Concrete - Part 2 : Slump Test. Brussels (2019). Comité Européen de Normalisation

[21] Comité Européen de Normalisation: NF EN 12390-3: Testing Hardened

Concrete - Part 3 : Compressive Strength of Test Specimens. Brussels (2019). Comité Européen de Normalisation

[22] Comité Européen de Normalisation: NF EN 12390-6: Testing Hardened Concrete - Part 6 : Tensile Splitting Strength of Test Specimens. Brussels (2012). Comité Européen de Normalisation

[23] Comité Européen de Normalisation: NF EN 12390-13: Testing Hardened Concrete - Part 13 : Determination of Secant Modulus of Elasticity in Compression. Brussels (2021). Comité Européen de Normalisation

[24] Association Française de recherches et d'essais sur les matériaux et constructions: APC-AFREM: Durabilité des Betons - Méthodes Recommandés Pour la Mesure des Granulats Associées a la durabilité. Toulouse (1997). Association Française de recherches et d'essais sur les matériaux et constructions

[25] Kollek, J.J.: The determination of the permeability of concrete to oxygen by the Cembureau method-a recommendation. Materials and Structures **22**(3), 225–230 (1989). https://doi.org/10.1007/BF02472192

[26] 116-PCD, R.T.: Permeability of concrete as a criterion of its durability. Materials and Structures **32**, 174–179 (1999)

[27] Klinkenberg, L.: The permeability of porous media to liquids and gases. In: Drilling and Production Practice, pp. 200–214 (1941). American Petroleum Institute

[28] Miah, M.J., Kallel, H., Carré, H., Pimienta, P., La Borderie, C.: The effect of compressive loading on the residual gas permeability of concrete. Construction and Building Materials **217**, 12–19 (2019). https://doi.org/10.1016/j.conbuildmat.2019.05.057

[29] Carré, H., Perlot, C., Daoud, A., Miah, M.J., Aidi, B.: Durability of ordinary concrete after heating at high temperature. In: Key Engineering Materials, vol. 711, pp. 428–435 (2016). Trans Tech Publ

[30] Truc, O., Ollivier, J.P., Carcassès, M.: A new way for determining the chloride diffusion coefficient in concrete from steady state migration test. Cement and Concrete Research **30**(2), 217–226 (2000). https://doi.org/10.1016/S0008-8846(99)00232-X

[31] Perlot, C., Verdier, J., Carcassès, M.: Influence of cement type on transport properties and chemical degradation: Application to nuclear waste storage. Materials and Structures/Materiaux et Constructions **39**(5), 511–523 (2006). https://doi.org/10.1617/s11527-005-9020-9

[32] Rozière, E., Loukili, A., Cussigh, F.: A performance based approach for durability of concrete exposed to carbonation. Construction and Building Materials **23**(1), 190–199 (2009). https://doi.org/10.1016/j.conbuildmat.2008.01.006

[33] Association Française de Normalization: XP P18-458: Essai Pour Béton Durci - Essai de Carbonatation Accélérée - Mesure de L'épaisseur de Béton Carbonaté. (2008). Association Française de Normalization

[34] Beushausen, H., Alexander, M.G., Basheer, M.G., Baroghel-Bouny, V., d'Andréa, R., Gonçalves, A., Gulikers, J., Jacobs, F., Khrapko, M., Monteiro, A.V., Nanukuttan, S.V., Otieno, M., Polder, R., Torrent, R.: Principles of the performance-based approach for concrete durability. In: Beushausen, H., Luco, L.F. (eds.) Performance-Based Specification and Control of Concrete Durability: Specifications State-of-the-Art Report RILEM TC 230-PSC, pp. 107–131. Springer, London (2016)

[35] Auroy, M., Poyet, S., Le Bescop, P., Torrenti, J.M., Charpentier, T., Moskura, M., Bourbon, X.: Comparison between natural and accelerated carbonation (3% CO2): Impact on mineralogy, microstructure, water retention and cracking. Cement and Concrete Research **109**, 64–80 (2018). https://doi.org/10.1016/j.cemconres.2018.04.012

[36] Castellote, M., Fernandez, L., Andrade, C., Alonso, C.: Chemical changes and phase analysis of OPC pastes carbonated at different CO2 concentrations. Materials and Structures/Materiaux et Constructions **42**(4), 515–525 (2009). https://doi.org/10.1617/s11527-008-9399-1

[37] Sisomphon, K., Franke, L.: Carbonation rates of concretes containing high volume of pozzolanic materials. Cement and Concrete Research **37**(12), 1647–1653 (2007). https://doi.org/10.1016/j.cemconres.2007.08.014

[38] Rougeau, P., Schmitt, L., Mai-Nhu, J., Djerbi, A., Sailio, M., Ghorbel, E., Mechling, J.M., Lecomte, A., Trauchessec, R., Bulteel, D., Cyr, M., Leklou, N., Amiri, O., Moulin, I., Lenormand, T.: Durability-related properties. In: de Larrad, F., Colina, H. (eds.) Concrete Recycling: Research and Practice, pp. 214–250. CRC Press, Boca Raton (2019)

[39] Mindeguia, J.-C., Pimienta, P., Carré, H., La Borderie, C.: On the influence of aggregate nature on concrete behaviour at high temperature. European Journal of Environmental and Civil Engineering **16**(2), 236–253 (2012). https://doi.org/10.1080/19648189.2012.667682

[40] Pimienta, P., Alonso, M.C., Jansson McNamee, R., Mindeguia, J.-C.: Behaviour of high-performance concrete at high temperatures: some highlights. RILEM Technical Letters **2**(2017), 45 (2017). https://doi.org/10.21809/rilemtechlett.2017.53

[41] Kwan, W.H., Ramli, M., Kam, K.J., Sulieman, M.Z.: Influence of the amount of recycled coarse aggregate in concrete design and durability properties. Construction and Building Materials **26**(1), 565–573 (2012). https://doi.org/10.1016/j.conbuildmat.2011.06.059

[42] Gonçalves, A., Esteves, A., Vieira, M.: Influence of recycled concrete aggregates on concrete durability. In: International RILEM Conference on the Use of Recycled Materials in Buildings and Structures, pp. 554–562 (2004). RILEM Publications SARL

[43] Kou, S.C., Poon, C.S.: Enhancing the durability properties of concrete prepared with coarse recycled aggregate. Construction and Building Materials **35**, 69–76 (2012). https://doi.org/10.1016/j.conbuildmat.2012.02.032

[44] Ghasemzadeh, F., Pour-Ghaz, M.: Effect of Damage on Moisture Transport in Concrete. Journal of Materials in Civil Engineering **27**(9), 04014242 (2015). https://doi.org/10.1061/(asce)mt.1943-5533.0001211

[45] Wang, L., Zhang, Q.: Investigation on water absorption in concrete after subjected to compressive fatigue loading. Construction and Building Materials **299**, 123897 (2021). https://doi.org/10.1016/j.conbuildmat.2021.123897

[46] Evangelista, L., de Brito, J.: Durability performance of concrete made with fine recycled concrete aggregates. Cement and Concrete Composites **32**(1), 9–14 (2010). https://doi.org/10.1016/j.cemconcomp.2009.09.005

[47] Gomes, M., De Brito, J.: Structural concrete with incorporation of coarse recycled concrete and ceramic aggregates: Durability performance. Materials and Structures/Materiaux et Constructions **42**(5), 663–675 (2009). https://doi.org/10.1617/s11527-008-9411-9

[48] Silva, R.V., Neves, R., De Brito, J., Dhir, R.K.: Carbonation behaviour of recycled aggregate concrete. Cement and Concrete Composites **62**, 22–32 (2015). https://doi.org/10.1016/j.cemconcomp.2015.04.017

[49] Dhir, R., Limbachiya, M., Leelawat, T.: Suitability of recycled concrete aggregate for use in bs 5328 designated mixes. Proceedings of the Institution of Civil Engineers-Structures and buildings **134**(3), 257–274 (1999)

[50] Kaid, N., Cyr, M., Julien, S., Khelafi, H.: Durability of concrete containing a natural pozzolan as defined by a performance-based approach. Construction and Building Materials **23**(12), 3457–3467 (2009). https://doi.org/10.1016/j.conbuildmat.2009.08.002

[51] San Nicolas, R., Cyr, M., Escadeillas, G.: Performance-based approach to durability of concrete containing flash-calcined metakaolin as cement replacement. Construction and Building Materials **55**, 313–322 (2014). https://doi.org/10.1016/j.conbuildmat.2014.01.063

[52] Idir, R., Cyr, M., Pavoine, A.: Investigations on the durability of alkali-activated recycled glass. Construction and Building Materials **236**, 117477 (2020). https://doi.org/10.1016/j.conbuildmat.2019.117477

[53] Bucher, R., Cyr, M., Escadeillas, G.: Performance-based evaluation of flash-metakaolin as cement replacement in marine structures – Case of chloride migration and corrosion. Construction and Building Materials **267** (2021). https://doi.org/10.1016/j.conbuildmat.2020.120926

[54] Association Française de Génie Civil: Conception des Bétons Pour Une Durée de Vie Donnée des Ouvrages – Maîtrise de la Durabilité Vis-à-vis de la Corrosion des Armatures et de L'alcali-réaction. Paris (2004). Association Française de Génie Civil